

# Magnetic Miniband Structure and Quantum Oscillations in Lateral Semiconductor Superlattices

M. Langenbuch,\* M. Suhrke, and U. Rössler

*Institut für Theoretische Physik - Universität Regensburg, 93040 Regensburg, Germany*

(Dated: January 10, 2022)

We present fully quantum-mechanical magnetotransport calculations for short-period lateral superlattices with one-dimensional electrostatic modulation. A non-perturbative treatment of both magnetic field and modulation potential proves to be necessary to reproduce novel quantum oscillations in the magnetoresistance found in recent experiments in the resistance component parallel to the modulation potential. In addition, we predict oscillations of opposite phase in the component perpendicular to the modulation not yet observed experimentally. We show that the new oscillations originate from the magnetic miniband structure in the regime of overlapping minibands.

PACS numbers: 73.20.At: Surface states, band structure, electron density of states, 73.23.Ad: Ballistic transport, 73.50.-h: Electronic transport phenomena in thin films.

Keywords: lateral superlattice, magnetic miniband structure, magnetotransport

## I. INTRODUCTION

The energy band structure of electrons in a periodic potential is one of the fundamental concepts in solid state physics. Developed in view of natural crystalline structures and in order to understand their electronic properties the concept of Bloch electrons applies as well to man-made periodic structures, which have become available with the advent of modern technological methods of growth and structuring [1, 2]. While in natural crystalline structures the lattice constant is fixed by the chemical binding mechanisms it can be varied over a wide range in superlattices produced by controlled technological processes. This development has renewed the interest in the challenging problem of *Bloch electrons in a magnetic field*, which was studied in the past by renowned theorists [3] but is experimentally accessible now with these artificial periodic structures, in which the lattice period  $a$  is in the same range as the classical cyclotron radius  $R_c$  at available magnetic fields.

Lateral superlattices are realized by applying lithographic techniques to impose a periodic pattern onto a two-dimensional electron system (2DES) at a semiconductor heterointerface [2]. This pattern can be an uni- or bi-directional potential modulation of different strength, thus allowing for a variety of artificial periodic structures. Magnetotransport experiments have become an efficient method for the investigation of the energy spectrum. At the beginning [4], with realizable periods  $a$  of these lateral superlattices (several 100 nm) much larger than the typical Fermi wavelengths  $\lambda_F$  of the 2DES (*e.g.* 50 nm), classical concepts have been successful in interpreting the magnetotransport data. One prominent example was the observation of  $1/B$  periodic oscillations in the low magnetic field range which could be ascribed to the commensurability condition  $2R_c = a(\nu - \frac{1}{4})$ ,  $\nu = 1, 2, 3, \dots$  [5]. With decreasing lattice periods (at present  $a \lesssim 100$  nm) quantum mechanical aspects gain importance. In fact, a new type of  $1/B$  periodic oscillations has been detected recently in lateral semiconductor superlattices with bi- [6] and uni-directional [7] electrostatic modulation. Their interpretation as being due to the formation of an artificial band structure was based on semiclassical arguments involving modifications of the Fermi contour of the 2DES by the superlattice potential and magnetic breakdown. It was possible to quantitatively relate the period of these novel quantum oscillations (including their dependence on electron density  $n_s$  and superlattice constant  $a$ ) to the area enclosed by the Fermi contours [6, 7, 8].

However, except for the magnetic breakdown this explanation did not address the combined effect of periodic potential and magnetic field that gives rise to a magnetic miniband structure.

In this letter we present fully quantum-mechanical magnetotransport calculations by evaluating Kubo's formula for a 2DES with non-perturbative treatment of both uni-directional periodic potential and magnetic field. It is shown that the new  $1/B$  periodic quantum oscillations reported in [6, 7] result from the formation of magnetic minibands which (at fixed magnetic field) evolve with increasing amplitude of the potential modulation from the Landau levels of the 2DES. Besides the impurity scattering, here considered in the self-consistent Born approximation (SCBA), it is the dispersion of these magnetic minibands, that determines the magnetoconductivity. As will be shown, both mechanisms

---

\*Electronic address: michael.langenbuch@physik.uni-regensburg.de

enter differently into the conductivities parallel and perpendicular to the potential modulation thus causing a phase shift by  $\pi$  in the novel quantum oscillations. The experimental detection of this phase shift together with the period of these magnetotransport oscillations can serve as evidence for the formation of magnetic minibands.

## II. MAGNETIC MINIBAND STRUCTURE

We consider electrons with effective mass  $m^*$  moving in the xy-plane subjected to a periodic electrostatic potential  $V(x) = \frac{V_0}{2} \cos\left(\frac{2\pi}{a}x\right)$ . The single-particle Hamiltonian is [9, 10, 11]

$$H = \frac{1}{2m^*} (\mathbf{p} + e\mathbf{A})^2 + V(x), \quad (1)$$

where the vector potential  $\mathbf{A}$  includes the magnetic field in z-direction and is given in Landau gauge by  $\mathbf{A}(x) = Bx\hat{\mathbf{e}}_y$ . The amplitude  $V_0$  of the potential modulation will be varied with respect to the Fermi energy  $E_F$  of the 2DES from weak ( $V_0 \ll E_F$ ) to strong ( $V_0 \lesssim E_F$ ). Due to the Landau gauge the Hamiltonian commutes with the  $y$ -component of the momentum. Without lateral superlattice ( $V_0 = 0$ ) the eigenstates can be characterized by two quantum numbers, the Landau level index  $n_L$  and the center coordinate  $X_0$ , which by  $X_0 = -\lambda_c^2 k_y$  is connected with the momentum  $\hbar k_y$  in  $y$ -direction ( $\lambda_c^2 = \hbar/eB$ ). In real space representation the eigenstates  $|n_L X_0\rangle$  are given by

$$\Psi_{n_L X_0}(x, y) = \varphi_{n_L}(x - X_0) \frac{1}{\sqrt{L_y}} e^{ik_y y} \quad (2)$$

where  $\varphi_{n_L}(\xi)$  is the eigenfunction of the harmonic oscillator and the energy eigenvalues  $E_{n_L} = \hbar\omega_c(n_L + \frac{1}{2})$ ,  $n_L = 0, 1, 2, \dots$  depend only on the Landau level index.  $\omega_c = \frac{eB}{m^*}$  is the cyclotron frequency. The spatial homogeneity of the unmodulated 2DES leads to a degeneracy of the Landau levels given by the ratio  $\Phi/\Phi_0$ , of the magnetic flux  $\Phi$  through the sample area  $L_x L_y$  and the elementary flux quantum  $\Phi_0 = h/e$ . When considering the superlattice potential this degeneracy is lifted and the Landau levels evolve into magnetic minibands described by a dependence of the energy eigenvalues on  $X_0$  (or  $k_y$ ), which due to the periodicity of the potential can be restricted to the interval  $[-\frac{a}{2}, \frac{a}{2}]$ .

The solution of the eigenvalue problem with  $H$  from Eq. (1) is the basis for the calculation of the magnetoconductivity. (In our calculations we have used the effective mass  $m^* = 0.067 m_0$ , typical for electrons in GaAs, the lattice constant  $a = 100$  nm, and the carrier density  $n_s = 2 \cdot 10^{15} \text{ m}^{-2}$  corresponding to  $E_F = 7.1$  meV). The energy spectrum at fixed magnetic field ( $B = 0.1$  T) is shown in Fig. 1 for two different strengths of the potential modulation  $V_0$  (left and right part).

For weak modulation ( $V_0 = 0.5$  meV) the Landau level structure can still be recognized, but the degeneracy is lifted already and gives rise to magnetic minibands with weak dispersion. With increasing  $V_0$  the dispersion gets stronger and the magnetic minibands overlap, thus the Landau level index loses its meaning and has to be replaced by the magnetic miniband index  $n$ . A striking feature of the magnetic miniband structure for strong modulation ( $V_0 = 2$  meV) are the sections with pronounced dispersion. Their classical analogue are channeling and drifting orbits [14]. These sections fall into limits defined by the dispersion of free and constantly Bragg reflected electrons [15].

In previous work [9, 10, 11] the potential modulation was treated as first order perturbation correction to the Landau levels. This treatment is justified if the potential modulation is much smaller than  $\hbar\omega_c$  and the minibands (Landau bands) still reflect the Landau level structure. This approach provided a quantum mechanical explanation of the commensurability oscillations as being due to the flat-band condition indicated by triangles in Fig. 1. In the quantum mechanical approach this condition can be formulated as  $R_c = \lambda_c^2 k$ , with  $k$  taken from the free electron dispersion relation  $E(k) = \frac{\hbar^2 k^2}{2m^*}$  and coincides with the maxima of the DOS-envelope. In this approach also the observed antiphase commensurability oscillations in the two diagonal resistivity components could be explained by invoking the two transport mechanisms due to Landau band dispersion and impurity scattering. However, first order perturbation theory is not adequate to describe the magnetotransport at very low magnetic fields, when the superlattice potential mixes the Landau levels into magnetic minibands.

## III. CONDUCTIVITY

Following a standard routine [11] we calculate the conductivity tensor in linear response theory by evaluating the Kubo formula [12, 13]:

$$\sigma_{\mu\nu} = \frac{ie^2\hbar}{L_x L_y} \int dE f_0(E) \left\langle \text{Sp} \left\{ v_\mu \frac{d\mathcal{G}^+}{dE} v_\nu \delta(E-H) - v_\mu \delta(E-H) v_\nu \frac{d\mathcal{G}^-}{dE} \right\} \right\rangle_I, \quad (3)$$

where  $v_\nu$  are the components of the velocity operator  $\mu, \nu \in \{x, y\}$ , and  $\mathcal{G}^\pm$  is the retarded (+) and advanced (−) Green function. The Fermi distribution  $f_0(E)$  includes the temperature and  $\langle \dots \rangle_I$  denotes an average over impurity configurations. This average is performed in SCBA by assuming short range scatterers. In the complex number approximation it yields a single-particle self-energy given by

$$\Sigma^+(E) = \Gamma^2 \sum_n \frac{1}{a} \int_{-a/2}^{a/2} dX_0 G_{nX_0}^+(E), \quad (4)$$

where  $\Gamma^2 = \frac{1}{2\pi} \hbar \omega_c \frac{\hbar}{\tau}$  is connected through the relaxation time  $\tau$  with the zero field mobility  $\mu = e\tau/m^*$ . The impurity average in Eq. (3) is considered by replacing  $\mathcal{G}^\pm$  by the impurity averaged Green functions  $G^\pm = \langle \mathcal{G}^\pm \rangle_I$ . Vertex corrections, which vanish in this approximation for the homogeneous 2DES, are neglected here. In the following we concentrate on the longitudinal conductivity  $\sigma_{\mu\mu}$  which can be written as:

$$\sigma_{\mu\mu} = \frac{e^2}{h} \frac{\hbar^2 \pi}{\lambda_c^2} \int dE \left( -\frac{df_0(E)}{dE} \right) \sum_{n_1, n_2} \frac{1}{a} \int_{-a/2}^{a/2} dX_0 |\langle n_1 X_0 | v_\mu | n_2 X_0 \rangle|^2 A_{n_1 X_0} A_{n_2 X_0}, \quad (5)$$

where  $n_1, n_2$  denotes the magnetic miniband index. The spectral functions  $A(E) = \frac{i}{2\pi} (G^+(E) - G^-(E))$  are obtained from the impurity averaged Green functions. In SCBA the density of states (DOS) can be expressed by:

$$D(E) = \frac{1}{L_x L_y} \text{tr}\{A(E)\} = -\frac{1}{(\pi \Gamma \lambda_c)^2} \text{Im} \{ \Sigma^+(E) \}. \quad (6)$$

The center part of Fig. 1 shows how  $D(E)$  evolves with increasing strength  $V_0$  of the potential modulation. Weak modulation ( $V_0 = 0.5$  meV) causes only a slight dispersion and the DOS with well separated peaks is still reminiscent of the Landau level structure of the homogeneous 2DES as indicated by dots. This characterizes the high-field regime of magnetotransport with the Shubnikov-de Haas (SdH) oscillations. With increasing modulation amplitude  $V_0$  the energy spectrum gets more complex until due to the strong coupling of Landau levels the DOS exhibits a new periodicity (indicated by the dots in the panel for  $V_0 = 2.0$  meV).

In a simple picture, neglecting in Eq. (5) the dependence of the matrixelement on quantum numbers, the conductivity is related to the DOS expressed by Eq. (6). Thus it is conceivable from the discussion of Fig. 1 that due to formation of magnetic minibands with strong dispersion novel  $1/B$  periodic quantum oscillations can show up with periods differing from those of commensurability and SdH oscillations.

In order to confirm this preliminary conclusion we turn now to the calculated conductivities perpendicular ( $\sigma_{yy}$ ) and parallel ( $\sigma_{xx}$ ) to the potential modulation as shown in Figs. 2 and 3, respectively.

The conductivities (for two different temperatures) are plotted here versus  $1/B$  to expose the characteristic periodicities. In the high field regime, when the potential modulation is much weaker than  $\hbar\omega_c$ , the conductivity is determined by the SdH oscillations characteristic for the Landau level spectrum. In the intermediate field regime the periods of the Weiss oscillations, determined by the commensurability condition, are marked for  $\sigma_{yy}$  (Fig. 2).

Oscillations with a new period  $\Delta_{1/B} = 0.37 \text{ T}^{-1}$  show up in both conductivity components in the low-field regime. It is characteristic for the new oscillations to vanish by increasing the temperature from 0.25 K (solid curves) to 2.0 K (dotted curves), while the Weiss oscillations can still be seen. In order to understand these results we consult Eq. (5). Contributions with  $n_1 \neq n_2$  are determined by the overlapping spectral functions from different magnetic minibands and will be called inter-miniband conductivity  $\sigma^{\text{inter}}$ . For weak modulation, when the overlap is caused exclusively by the SCBA broadening alone, this contribution can be ascribed to impurity scattering and is also called scattering conductivity [9, 10, 11]. The second mechanism deriving from terms with  $n_1 = n_2$  is due to the dispersion of the magnetic minibands exclusively (the matrixelements in Eq. (5) correspond to the group velocity) and will be called intra-band conductivity  $\sigma^{\text{intra}}$ . For systems with uni-directional potential modulation in  $x$  direction the matrixelement  $\langle nX_0 | v_x | nX_0 \rangle$  vanishes and the intra-band conductivity contributes only to  $\sigma_{yy}$ . Thus the use of 1D lateral superlattices permits the observation of quantum oscillations of scattering and band contributions to the conductivity at the same time. Note that up to present quantum oscillations in the 1D case [7] have been found only in the magnetoresistance parallel to the modulation which corresponds to the perpendicular conductivity. As can be seen in Fig. 3,  $\sigma_{xx}$  is almost identical (in magnitude and phase) with  $\sigma_{yy}^{\text{inter}}$  except for the low field regime where the new oscillations occur. We focus our attention to this regime and to the new oscillations by showing in Fig. 4 the difference between the conductivities calculated for the two temperatures. As can be seen clearly  $\Delta\sigma_{xx} = \sigma_{xx}(0.25 \text{ K}) - \sigma_{xx}(2.0 \text{ K})$  and  $\Delta\sigma_{yy}$  oscillate in antiphase. This is a consequence of the two mechanisms (inter- and intra- miniband) contributing differently to the conductivity parallel and perpendicular to the potential modulation and thus reflects the formation of magnetic minibands:  $\sigma_{xx}$  is dominated by inter-miniband contributions

with maxima correlated with those of the DOS;  $\sigma_{yy}$  is dominated (for the parameters used here) by intra-miniband contributions, that get large when parts of the magnetic miniband with strong dispersion, which correspond to small DOS, pass through the Fermi energy. A similar explanation has been invoked to explain the observed antiphase in commensurability oscillations yet under the assumption of weak modulation and only slightly distorted Landau band spectrum [9, 10, 11]. Here we provide more rigorous analysis for arbitrary modulation strength (or low magnetic field) at which the new  $1/B$  periodic oscillations appear which together with the antiphase signature, if observed experimentally, can be taken as a proof for the formation of the magnetic minibands in 2DES with uni-directional potential modulation. In general, as the oscillations have been observed for 2D modulated systems too [6], the periodicity of the quantum oscillations can be explained by the density of states but the phase depends on the dominating conductivity mechanism.

#### IV. SUMMARY

In conclusion we address one of the challenging single-particle problems in solid state physics: Bloch electrons in a magnetic field and a possible proof of the formation of a magnetic band structure. For this purpose we perform a quantum-mechanical calculation of the magneto conductivity by evaluating the Kubo formula for a system of 2D electrons with an uni-directional periodic potential modulation in an external homogeneous magnetic field included non-perturbatively. Such systems are realized nowadays in layered semiconductor structures with modern technologies of growth and lithography. It is shown that the formation of a magnetic miniband structure together with the impurity scattering manifests in the magneto conductivities parallel and perpendicular to the potential modulation: in the low magnetic field regime new  $1/B$  periodic quantum oscillations show up, which are in antiphase for the two longitudinal components of the conductivity tensor due to different conductivity mechanisms and should be observable only at very low temperatures.

This work has been supported by the DFG via Forschergruppe 370 *Ferromagnet-Halbleiter-Nanostrukturen*.

- 
- [1] *Electronic Properties of Multilayers and Low-Dimensional Semiconductor Heterostructures* edited by J.M. Chamberlain, et al., Nato ASI Series B **231**, Plenum Press, NewYork (1990).
  - [2] D. Weiss, Adv. Sol. Stat. Phys. **31**,341 (1991).
  - [3] P. Peierls, Z. Phys. **80**, 763 (1933); L. Onsager, Phil. Mag. **43**, 1006, (1952); A.B. Pippard, Proc. Roy. Soc. (London) A **270**, 1 (1962); G.H. Wannier Rev. Mod. Phys. **34**, 645 (1962); E. Brown Phys. Rev. **133**, A1038 (1964); W.G. Chambers Phys. Rev. **140**, A135 (1965).
  - [4] D. Weiss, K. von Klitzing, K. Ploog, and G. Weimann, Europhys. Lett. **8**, 179 (1989); R.W. Winkler, J.P. Kotthaus, and K. Ploog, Phys. Rev. Lett. **62**, 1177 (1989).
  - [5] C.W.J. Beenakker, Phys. Rev. Lett. **62**, 2020 (1989).
  - [6] C. Albrecht, et al., Phys. Rev. Lett. **83**, 2234 (1999).
  - [7] R.A. Deutschmann, et al., Phys. Rev. Lett. **86**, 1857 (2001).
  - [8] M. Langenbuch, et al., Physica E**6**, 565 (2000).
  - [9] R.R. Gerhardt, D. Weiss, and K. von Klitzing, Phys. Rev. Lett. **62**, 1173, (1989).
  - [10] P. Vasilopoulos and F .M. Peeters, Phys. Rev. Lett. **63**, 2120 (1989).
  - [11] C. Zhang and R.R. Gerhardt Phys. Rev. B **41**, 12850, (1990).
  - [12] P. Strěda and L. Smrčka, Phys. Stat. Sol (b) **70**, 537 (1975).
  - [13] R. Kubo, J. Phys. Soc. Japan **12**, 570 (1957).
  - [14] S.D.M.Zwerschke, et. al., Phys. Rev. B. **60**, 5536 (1999).
  - [15] Due to the modulation so called channeling orbits exist whose energies are not quantized in the magnetic field. By avoiding bandcrossings the continuous energy dispersion and the discrete energies of the Landau ladder form the magnetic miniband structure for high  $V_0$ . The energy dispersions of electron waves moving straight in y-direction,  $E(k) = \frac{\hbar^2 k^2}{2m^*}$ , and of wave packets consisting of electrons which are Bragg reflected at  $k_x = \frac{\pi}{a}$ ,  $E(k) = \frac{\hbar^2 k^2}{2m^*} - \frac{1}{12} \frac{\hbar^2 \pi^2}{m^* a} \ln(1 + 6 \frac{k^2 a^2}{\pi^2})$ , are marked in Fig. 1(right). These limits separate the dispersive part of the magnetic minibands from the flat one for our parameters. Note that the Bragg reflected wave is no classical path in contrast to the trajectories considered in [14] to explain the miniband structure.

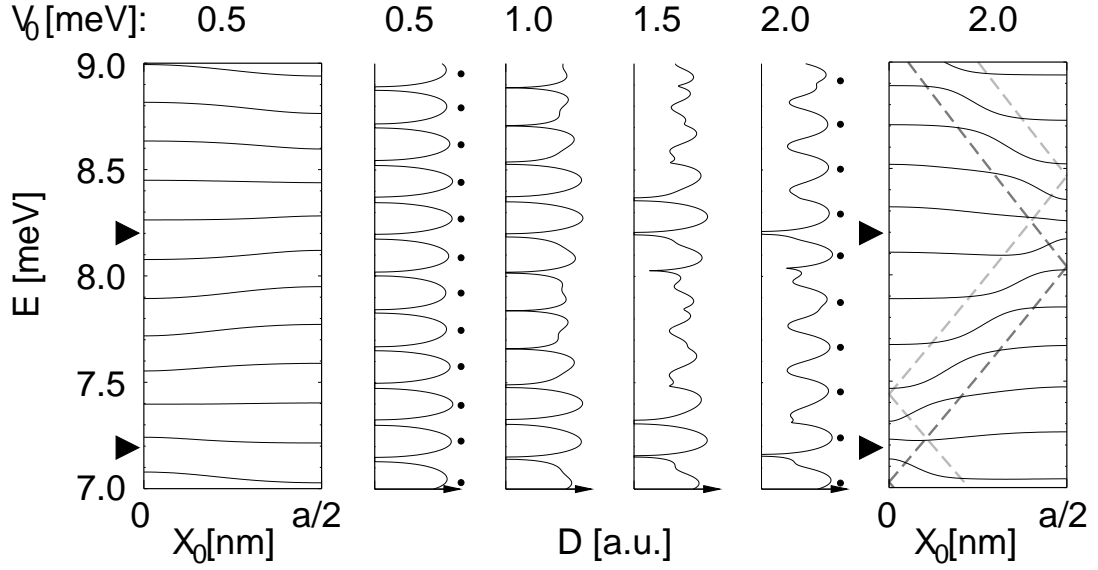


FIG. 1: Part of the magnetic miniband structure (left and right) and density of states  $D(E)$  (center) for uni-directional modulation with  $a = 100$  nm,  $\mu = 50$  m<sup>2</sup>/Vs,  $m^* = 0.067 m_0$  and different modulation amplitudes  $V_0$  at a magnetic field  $B = 0.10$  T. The maxima of the density of states are marked for  $V_0 = 0.5$  meV and  $V_0 = 2.0$  meV. The dashed lines in the miniband structure for  $V_0 = 2.0$  meV is the dispersion of free (light grey) and constantly Bragg reflected electrons (dark grey) [15]. The triangles at the energy axes mark the flat-band conditions.

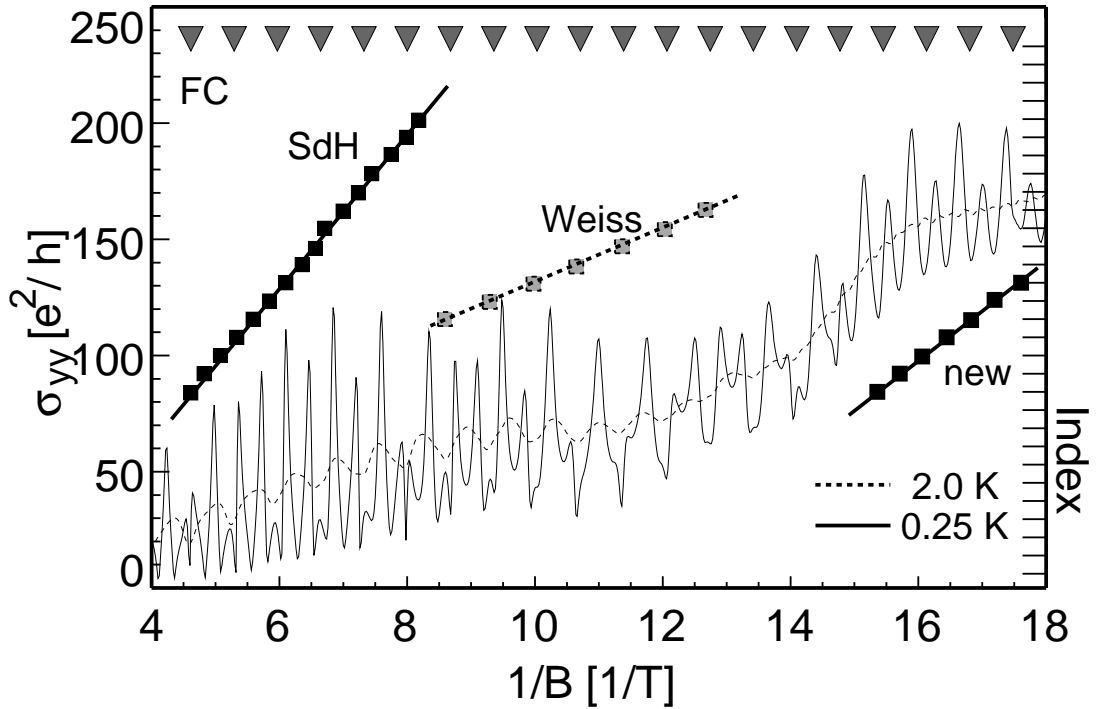


FIG. 2: Conductivity  $\sigma_{yy}$  perpendicular to the modulation direction at  $T = 2.0$  K (dotted curve) and  $0.25$  K (solid curve) for an uni-directional modulation with  $V_0 = 2.0$  meV and  $a = 100$  nm. The electron system is characterized by  $m^* = 0.067 m_0$ ,  $\mu = 50$  m<sup>2</sup>/Vs and  $n_s = 2.0 \cdot 10^{15}$  m<sup>-2</sup>. The flat-band conditions are marked by triangles. The  $1/B$  periodicities of SdH  $\Delta_{1/B} = 0.24$  T<sup>-1</sup>, commensurability (Weiss)  $\Delta_{1/B} = 0.68$  T<sup>-1</sup> and new quantum oscillations  $\Delta_{1/B} = 0.37$  T<sup>-1</sup> are indicated, by assigning an index to the position of the minima in the calculated conductivity. For the commensurability oscillations the minima at  $T = 2.0$  K are taken.

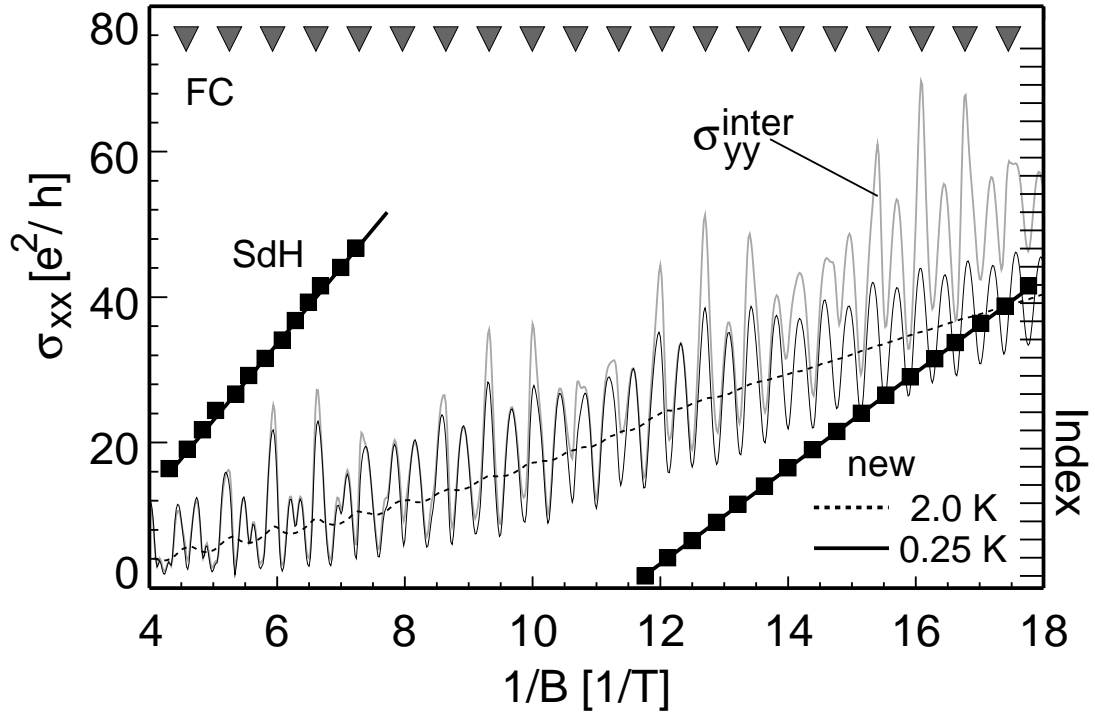


FIG. 3: Same as Fig. 2 but conductivity  $\sigma_{xx} = \sigma_{xx}^{inter}$  parallel to the modulation is shown. For comparison we plot  $\sigma_{yy}^{inter}$ , the inter-miniband contribution to  $\sigma_{yy}$ . The flat-band conditions (FC) are marked by triangles. The  $1/B$  periodicities of SdH oscillations and of the new quantum oscillations (new) are indicated.

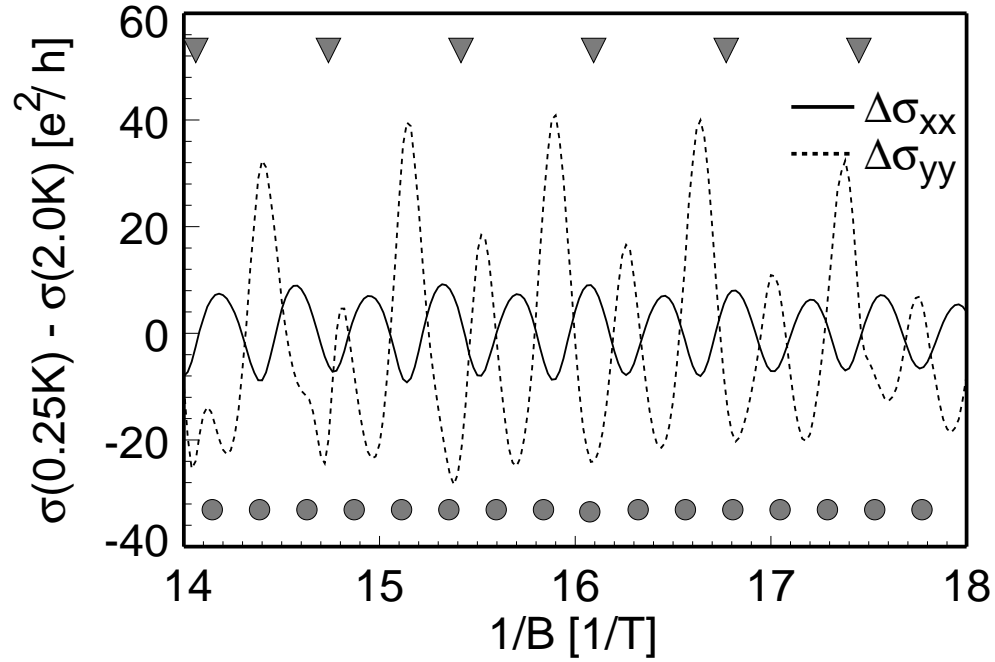


FIG. 4: Difference of the longitudinal conductivities at 0.25 K and 2.0 K with the parameters of Fig. 2. The flat-band conditions are marked by triangles and the expected SdH maxima by grey bullets.